J. Fluid Mech. (1986), *vol.* 167, *pp.* 393–407
Printed in Great Britain

Moving contact lines at non-zero capillary number

By KALVIS M. JANSONS†
Department of Applied Mathematics and Theoretical Physics,
University of Cambridge, Silver Street, Cambridge CB3 9EW

(Received 18 December 1984 and in revised form 15 November 1985)

Consider the unsteady motion of a fluid–fluid interface over and attached to a solid surface with one-dimensional periodic roughness in the limit of small capillary number $\mathbb{C}$. We show that the macroscopic behaviour of the interface can be described, to leading order in $\mathbb{C}$, in terms of well-defined continuum quantities, even though the complicated fluid motion in the neighbourhood of the contact line cannot. The key is that contact-angle hysteresis makes it possible to isolate the viscous stress singularity at the contact line, since for a sufficiently slowly moving fluid–fluid interface all the movement of the contact line occurs in a time much shorter than the macroscopic timescale. The effective 'slip length' for the macroscopic description is shown to be velocity dependent and equal to $a\mathbb{C}^{-1}$, where a is the wavelength of the roughness on the solid surface. Finally, we consider surfaces with two-dimensional random roughness, and argue that they too would exhibit velocity dependent 'slip lengths', though the velocity dependence would be stronger in this case. These results combined with earlier work (Jansons 1985) explain why observed 'slip lengths' can be much larger than roughness dimensions, and why the degree of 'stick-slip' decreases with increasing speed.

1. Introduction

Consider the unsteady motion of a fluid–fluid interface between immiscible fluids over a solid surface with one-dimensional periodic roughness in the limit where, on a macroscopic scale, surface-tension forces dominate over viscous forces. The aim is to determine how the non-integrable stress singularity at the contact line of the three phases in the Navier–Stokes description of the motion (with a condition of no-slip at solid boundaries) might be removed from the macroscopic description. The idea that roughness is important in the renormalization of the viscous stress singularity is not new (Hocking 1977, for example), however the importance of unsteadiness has been overlooked. If unsteadiness is ignored, Hocking (1977) found that the cutoff distance for the viscous stress singularity is of the order of roughness dimensions; though, in fact, unsteadiness is vital.

A great deal of work has been done in the field of 'moving contact lines', and is reviewed by Dussan V. (1979). However, removal of the viscous stress singularity has been *ad hoc*. The cutoff distance of the viscous stress singularity, which is often called a 'slip length' (Dussan V. 1976), is shown to be dependent on the speed of the contact line through the unsteadiness of the motion. We assume that the Navier–Stokes equation with a condition of no-slip is not valid in the neighbourhood of the contact line, and that there is some mechanism, on a microscopic scale by which contact lines can move. However, details of this mechanism *do not* determine in *any way* the leading-order solution for the macroscopic flow field, *nor* the effective 'slip length'.

† From September 1986: Department of Mathematics, University College London, Gower Street, London WC1E 6BT.

The mechanism of contact-line motion is important only in determining the error terms and range of validity of the solution, and *not* the form of the solution.

One key idea is that the unsteady motion in the neighbourhood of the contact line is driven by the energy that is implicit in the contact-angle hysteresis, where contact-angle hysteresis is the phenomenon that the apparent angle of contact of the fluid–fluid interface with the solid surface is a discontinuous function of the direction of motion. Thus we expect the results to generalize to all types of rough surface, since in practice all rough surfaces exhibit contact-angle hysteresis.

Throughout we consider the simplest systems that exhibit the physical effects of interest to highlight the important mechanisms, particularly the importance of unsteadiness. We shall restrict attention to systems of negligible inertia (i.e. zero Reynolds number). Though surfaces with one-dimensional roughness are not realistic and can exhibit quite different wetting behaviour from surfaces with two-dimensional random roughness (Jansons 1985), in §5 we argue that in this case we do expect similar results. However, the precise velocity dependence of the effective 'slip length' is different.

We begin in §2 by considering the viscous stress singularity and estimate the timescale for contact-line movement. This estimate is used in following sections to determine the range of validity of the analysis and the sizes of neglected effects. The lengthscale on which the continuum approximation breaks down does not appear in the results for a sufficiently 'slowly moving' contact line. So this section is included only for completeness, since for following sections we need only that contact lines can move (somehow) to determine the macroscopic flow field to leading order.

In §3 we consider the time evolution of the fluid–fluid interface close to the contact line as the contact line moves over the rough solid surface. A similarity solution is found for the relaxation process of the fluid–fluid interface under the action of surface tension.

In §4 the results of the previous sections are combined to determine the way in which a fluid–fluid interface with a 'slowly moving' contact line moves over a solid surface with one-dimensional periodic roughness. We find a natural way to define a renormalized macroscopic description (regular at the contact line) from which an effective 'slip length' is calculated; the key is the similarity solution of §3. The 'slip length' determined is aC^{-1}, where a is the wavelength of the roughness and C the capillary number, i.e. the ratio of viscous forces to surface-tension forces.

Finally, in §5, we discuss the difference between the behaviour of a fluid–fluid interface moving over solid with one-dimensional periodic roughness and two-dimensional random roughness of the type considered by Jansons (1985). It is argued that the 'slip length' for two-dimensional random roughness is more velocity-dependent. We also explain why the size of the jumps in the 'stick-slip' motion of the contact line decreases with increasing speed.

2. The viscous stress singularity

The first difficulty encountered when solving a problem that involves a moving contact line on a perfectly flat surface is that the stress as given by the Navier–Stokes equation has a non-integrable singularity at the contact line due to the no-slip boundary condition (Dussan V. 1979). We shall discuss briefly why this singularity is present, and make estimates for use in following sections. In following sections we do not require a detailed analysis of the stress singularity at the contact line, only that contact lines can move. *These estimates are important only in determining the range* *of validity and error terms of the results.* (Any reader already happy with the fact that contact lines can move, and able to estimate the rate of movement, should skip this section.)

The stress, which grows like r^{-1} (where r is the distance from the contact line), cannot be an accurate model on lengthscales where the continuum approximation breaks down. Define δ to be the lengthscale of the neighbourhood of the contact line on which the stress singularity is renormalized microscopically. In the analysis of this paper the value of δ does not enter into the solution for sufficiently slowly moving contact lines on a rough surface, and only $\log \delta$ appears in the error terms and conditions of validity. (For this reason we keep an open mind as the value of δ).

A lower bound for δ is molecular size, since it is clear that there is no mechanism by which a macroscopically observable stress can continue to grow on smaller lengthscales. An upper bound is the lengthscale of the longest-range forces implicitly included in continuum models, namely dispersion (or van der Waals) forces.

2.1. *Calculation of the contact-line jump time for a periodic solid surface*

We now establish what is meant by 'slowly moving' for use in following sections: A sufficiently slowly moving contact line on a solid surface with one-dimensional periodic roughness does not move at a constant speed (Jansons 1985), but jumps from one position to another, where it remains almost stationary until the next jump. A useful definition of the term 'slowly moving' therefore is the ratio of the time taken for a rapid jump to the time taken for the whole interface to move the same distance. We assume that the slow movement of the fluid–fluid interface many roughness dimensions away from the contact line (necessary to trigger the rapid jump) is negligible during the jump itself. Though the estimates made are valid for a variety of periodic surfaces, it is useful to begin with a very simple example to highlight the important physical processes.

Consider a one-dimensional period solid surface of wavelength a that is flat except for thin ridges (or grooves) as shown in figure 1. We assume that all roughness dimensions are large compared with the cutoff length δ, and that there is a well-defined microscopic static contact angle θ_{mic}, for a contact line that has moved in only one direction (Jansons 1985). The microscopic static contact angle is the angle that the fluid–fluid interface makes with the tangent plane of the solid surface.

Take the position of the contact line just before the jump as $z = 0$ (represented by A in figure 1), where z is the Cartesian coordinate along the solid surface in the direction of motion of the contact line. To simplify the analysis assume that the angle of the slope α of the solid surface at the point marked A is such that $\theta_{\text{mic}} + \alpha$ is well within the range 0 to π, since this avoids unnecessary complications (Jansons 1985).

We may now calculate the magnitude of the time taken for the contact line to move from point A to that marked B (in figure 1) on the next ridge. When the contact line breaks from A the fluid–fluid interface is out of equilibrium, since there is a net surface-tension driving force per unit width of the contact line equal to

$$\gamma[\cos \theta_{\text{mic}} - \cos(\theta_{\text{mic}} + \alpha)], \tag{2.1}$$

which is balanced by viscous resistance. This resistance can be estimated from the solution of the classical corner-flow cutoff at distance δ from the contact line, namely

$$\mu U_{\text{jump}}(z) \log\left(\frac{H(z)}{\delta}\right), \tag{2.2}$$

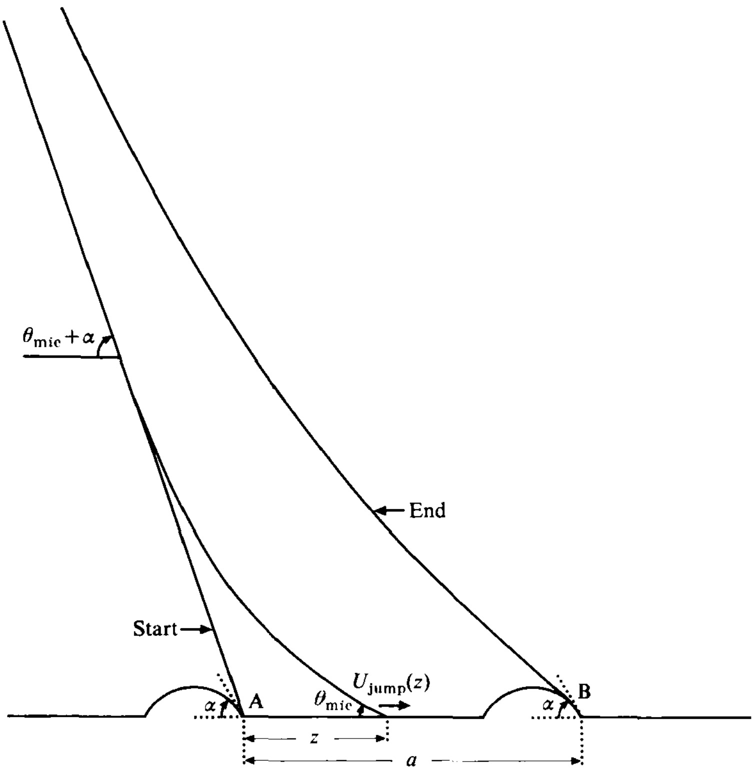

FIGURE 1. Defining diagram for contact-line jump process.

where $H(z)$ is the vertical scale of the curved part of the fluid–fluid interface, μ is a typical viscosity, and $U_{\text{jump}}(z)$ is the speed of the contact line. We also assume that the contact angle during the jump is the same to an order of magnitude as the static contact angle. Since $H(z) \approx z$ (where '$\approx$' means equal to an order of magnitude), combining (2.1) and (2.2) we find

$$\gamma[\cos\theta_{\text{mic}} - \cos(\theta_{\text{mic}}+\alpha)] \approx \mu U_{\text{jump}}(z)\log\left(\frac{z}{\delta}\right). \tag{2.3}$$

From (2.3) we find an expression for the time T_{jump} for the contact line to reach the next ridge at point B (in figure 1), namely

$$\gamma\int_0^{T_{\text{jump}}}[\cos\theta_{\text{mic}} - \cos(\theta_{\text{mic}}+\alpha)]\,\mathrm{d}t \approx \mu\int_0^a \log\left(\frac{z}{\delta}\right)\mathrm{d}z. \tag{2.4}$$

Hence
$$T_{\text{jump}} \approx \frac{a\mu}{\gamma}\frac{\log\left(\frac{a}{\delta}\right)}{[\cos\theta_{\text{mic}} - \cos(\theta_{\text{mic}}+\alpha)]}, \tag{2.5}$$

where we have neglected the order-unity terms as compared with $\log(a/\delta)$.

If the fluid–fluid interface far away from the contact line is moving with speed U, the macroscopic (or mean) time T_{macro} for the interface to move over one wavelength of the solid surface is

$$T_{\text{macro}} = \frac{a}{U}. \tag{2.6}$$

Thus the 'slowness parameter' ϵ, which is the ratio of the time for microscopic contact-line movement to the mean time for the fluid–fluid interface to move one wavelength, is

$$\epsilon = T_{\text{jump}}/T_{\text{macro}}$$
$$= C\frac{\log\left(\dfrac{a}{\delta}\right)}{\cos\theta_{\text{mic}} - \cos\left(\theta_{\text{mic}}+\alpha\right)}, \tag{2.7}$$

where $C = \mu U/\gamma$ is the (macroscopic) capillary number.

We assume that ϵ is much less than unity, which gives the following condition on the capillary number:

$$C \ll \frac{\cos\theta_{\text{mic}} - \cos\left(\theta_{\text{mic}}+\alpha\right)}{\log\left(\dfrac{a}{\delta}\right)}. \tag{2.8}$$

Note that (2.8) is stronger than the usual condition $C \ll 1$ for other problems where surface tension dominates viscous forces. This analysis becomes invalid for all values of C on a perfectly flat solid surface (where $\alpha = 0$), since the right-hand side of (2.8) is zero. In this case the details of the motion on a lengthscale δ of the contact line are always important, and beyond the scope of this paper. However, Jansons (1985) showed that even small amounts of roughness can give a large perturbation to the contact angle.

The condition (2.8) on C is appropriate for many other types of solid surface with one-dimensional periodic roughness; for example a sinusoidal surface where the contact line jumps from the point of maximum down slope to an equivalent position one wavelength ahead.

3. The relaxation process of a fluid–fluid interface

Consider the evolution of a fluid–fluid interface that is flat and perpendicular to a plane solid surface except for a region in the neighbourhood of the contact line (see figure 2). In this neighbourhood the fluid–fluid interface is displaced forward beyond its mean level and relaxes under the action of surface tension γ alone. The viscosities of the two fluids are assumed equal, which simplifies the analysis but does not significantly affect the physics (Rallison & Acrivos 1978). In figure 2 the solid line represents the initial position of the fluid–fluid interface and the dotted line the final (or asymptotic) position, where the entire interface has relaxed. However, convergence to the dotted line is pointwise rather than uniform in y. The results of this section will be used in §4, to model the motion of the interface in the neighbourhood of the contact line, where we do not need to know the behaviour accurately for short times (when the equations of motion are nonlinear). Thus we restrict our attention to the limit of large time.

To derive the linearized governing equations for the fluid–fluid interface we first consider the full nonlinear description. The evolution equation for a three-dimensional fluid–fluid interface S driven by surface tension at zero Reynolds number for an unbounded fluid, i.e. no solid boundaries (Rallison & Acrivos 1978), is given by

$$\boldsymbol{u}(\boldsymbol{x}) = \int_S \boldsymbol{J}_3(\boldsymbol{x}-\boldsymbol{y})\cdot\gamma\kappa(\boldsymbol{y})\,\boldsymbol{n}(\boldsymbol{y})\,\mathrm{d}S_y, \tag{3.1}$$

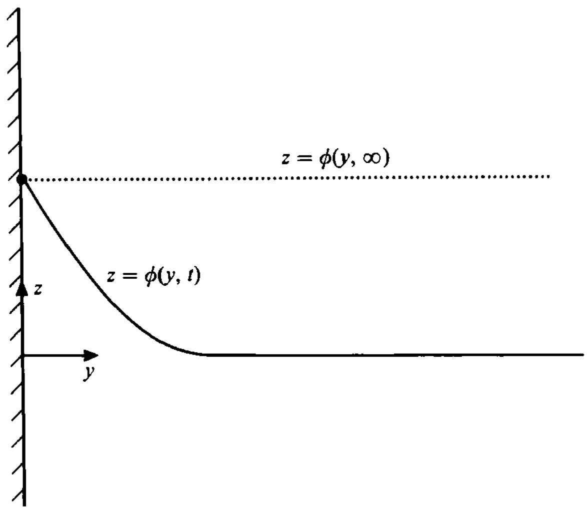

FIGURE 2. Defining diagram for the relaxation process.

where $\boldsymbol{u}(\boldsymbol{x})$ is the velocity of the interface at a point $\boldsymbol{x}, \gamma\kappa(\boldsymbol{y})\,\boldsymbol{n}(\boldsymbol{y})$ is the stress jump across the interface (with curvature $\kappa(\boldsymbol{y})$ and normal $\boldsymbol{n}(\boldsymbol{y})$) at point $\boldsymbol{y}$ and

$$\boldsymbol{J}_3(\boldsymbol{r}) = \frac{1}{8\pi\mu r}\left(1+\frac{\boldsymbol{rr}}{r^2}\right) \tag{3.2}$$

is the Green function for Stokes flow (Batchelor 1967) where $\boldsymbol{r} = \boldsymbol{x}-\boldsymbol{y}, r = |\boldsymbol{r}|$ and μ is the viscosity of both fluids. The boundary condition at infinity in the analysis of Rallison & Acrivos (1978) was that the velocity field tended to a linear ambient flow. However, we assume that the fluid velocity tends to zero as r tends to infinity.

To derive the evolution equation for a fluid–fluid interface over an infinite solid plane boundary with a condition of no-slip at its surface, we must add to (3.1) terms to include the image system of Blake (1971). The image system for a point force (or Stokeslet) of strength s, and perpendicular height h above the solid surface consists of an equal and opposite Stokeslet, a Stokes-doublet of strength $2hs$ and a source-doublet of strength $2h^2s$ all at the image point. This implies that the flow $\boldsymbol{u}(\boldsymbol{x})$ above the plane, with normal $\boldsymbol{m}$, driven by a Stokeslet $\boldsymbol{s}$, at $\boldsymbol{y}$, is given by

$$\boldsymbol{u}(\boldsymbol{x}) = \boldsymbol{s}\cdot\left\{\boldsymbol{J}_3(\boldsymbol{r})-\boldsymbol{J}_3(\boldsymbol{R})+2h(1-2\boldsymbol{mm})\cdot\frac{\partial}{\partial \boldsymbol{R}}\left\{\frac{h\boldsymbol{R}}{8\pi\mu R^3}-\boldsymbol{J}_3(\boldsymbol{R})\cdot\boldsymbol{m}\right\}\right\}, \tag{3.3}$$

where $\boldsymbol{r} = \boldsymbol{x}-\boldsymbol{y}$ and $\boldsymbol{R} = \boldsymbol{x}-\boldsymbol{y}+2\boldsymbol{mm}\cdot\boldsymbol{y}$.

From (3.2) we can find the corresponding Green function for the two-dimensional system by integration from $-\infty$ to $+\infty$ in the redundant variable, giving

$$\boldsymbol{J}_2(\boldsymbol{r}) = \frac{1}{4\pi\mu}\left[\log\left(\frac{1}{r}\right)1+\frac{\boldsymbol{rr}}{r^2}\right], \tag{3.4}$$

where $\boldsymbol{r}$ now refers to the two-dimensional system. Though the two-dimensional Green function is unbounded as r tends to infinity for an unbounded system, the addition of an infinite solid plane boundary has the effect of renormalizing the far field, which is that of a Stokes-doublet.

Integrating (3.3) and defining the fluid–fluid interface at time t by $z = \phi(y, t)$ where

y and z are the Cartesian coordinates perpendicular to and along the solid surface, we find the linearized two-dimensional equation

$$\dot{\phi}(y,t) = \frac{\gamma}{4\pi\mu}\int_0^\infty G\left(\frac{y}{h}\right)\phi_{hh}(h,t)\,\mathrm{d}h, \tag{3.5}$$

where $\dot{}$ denotes a time and subscript a space derivative, and

$$G\left(\frac{y}{h}\right) = \log\left|\frac{y+h}{y-h}\right| - \frac{2hy}{(y+h)^2}. \tag{3.6}$$

Equation (3.5) has a similarity solution of the form $\phi(y,t) = \phi(y/t, 1)$, where we have taken the time t corresponding to the initial condition equal to 1. It can be shown (Appendix A) that the long-time solution for any initial condition of (3.5) resulting from the rapid jump of the contact line tends to a similarity solution of this form. This can be argued informally by extrapolating the similarity solution back to $t = 0$, where its initial condition is a Heaviside unit function. Since any initial condition being considered will appear to be a Heaviside unit function on some horizontal scale (or resolution), on the same scale the solution will be given approximately by the similarity solution for later times. The structure on smaller lengthscales will die away owing to the smoothing action of surface tension.

To determine the similarity solution define $Y = \mu y/\gamma t$, $H = \mu h/\gamma t$ and $f(y) = (\mathrm{d}/\mathrm{d}Y)\,\phi(Y,1)$. Then from (3.5) we find

$$-Yf(Y) = \frac{1}{4\pi}\int_0^\infty G\left(\frac{Y}{H}\right)\frac{\mathrm{d}f}{\mathrm{d}H}(H)\,\mathrm{d}H, \tag{3.7}$$

which can be solved numerically to give a solution of the form

$$\phi(y,t) = F\left(\frac{\mu y}{\gamma t}\right), \tag{3.8}$$

where F is a non-dimensional function of a non-dimensional argument, with $F(0) = 1$ and $F(x) \to 0$ as $x \to \infty$. Since in §4 we do not require the similarity solution F itself, but rather an infinite sum of such solutions, we shall not discuss the numerical results here.

4. Motion of a fluid–fluid interface over a periodic solid surface

Consider the motion of a fluid–fluid interface over a periodic solid surface in the limit of small ϵ (i.e. where the timescale for rapid jumps is much shorter than that for the whole interface to move); later we also determine a lower bound on ϵ. In this section, since we are interested only in the leading-order terms, the behaviour of the fluid–fluid interface on a timescale T_{jump} is of no importance; though we assume contact lines can move. We also assume that the macroscopically apparent speed U of the contact line is constant; however, this condition is relaxed later.

In §3 the motion of the fluid–fluid interface for a system that is at rest, except for the motion due to the rapid jump, was described by a similarity solution in the limit of large time. However, for a system in steady motion far from the contact line, the total velocity field includes a contribution from each of the similarity solutions due to each of the rapid jumps that have occurred.

4.1. *The problem to be solved*

We can now pose the problem that we need to solve in order to determine the motion of the fluid–fluid interface (to leading order in ϵ) on a lengthscale much less than macroscopic dimensions. From the solution we can derive the matching condition for a macroscopic flow problem with a contact line moving over a solid surface with one-dimensional periodic roughness. We assume that a mechanism for a 'rapid jump' of the contact line exists without stating the precise nature of this motion, and later we show that the solution is independent of the particular mechanism. This implies that, though the estimates for the error terms and the range of validity are *ad hoc*, the final solution (to leading order) is well defined.

Since we are interested only in a leading-order solution in ϵ, we may again use linearized equations. We must find a solution of (3.5) that satisfies the boundary conditions for the rapid jump, namely one that has the correct contact angle at the moment just before the jump takes place. For algebraic simplicity we take the contact angle just before the jump as $\frac{1}{2}\pi$. We also require a boundary condition at inifinity, or more precisely, we need the correct asymptotic form for the interface shape in the limit of large y. Finally, the required solution must be periodic, in the sense that after a time a/U the fluid–fluid interface must return to its initial position except for a translation of magnitude a in the direction of motion.

The boundary condition for large y requires some thought. However, this has already been discussed in detail by Dussan V. (1976), and we shall refer to her work later in this section.

To solve this problem, we first make an intelligent guess at the solution, and then prove that this solution is correct and satisfies the boundary conditions.

4.2. *The time-dependent fluid–fluid interface shape*

Consider the sum of the similarity solutions for all the rapid jumps that have occurred if the contact line has been moving in the same direction for a long time; later, this time is estimated. If the sum is taken naively it is divergent; however, we may add a linear term to each of the similarity solutions without changing their time-dependence. This can be done to satisfy the boundary conditions at the contact line at the instant just before the next rapid jump: thus

$$\phi(y,t;C) = a\sum_{n=1}^{\infty}\left[F\left(\frac{y}{\gamma t/\mu+naC^{-1}}\right)-F'(0)\frac{y}{naC^{-1}-1}\right]+aF\left(\frac{\mu y}{\gamma t}\right), \tag{4.1}$$

for $0 \leqslant t < a/U$. Since each term in (4.1) is a solution to the governing equation (3.5), then so too is the sum, since this equation is linear. The boundary conditions are also linear to the same order of approximation, since they are applied at a plane $z = \text{constant}$ (for simplicity taken as zero). We now show that (4.1) satisfies all the other boundary conditions, namely that it has the correct behaviour for large y and is periodic in the sense described earlier.

Proof that the solution is periodic

Consider

$$\phi\left(y,\frac{a}{U};C\right)-\phi(y,0;C) = a\lim_{N\to\infty}\sum_{n=1}^{N}\left[F\left(\frac{y}{(n+1)aC^{-1}}\right)-F\left(\frac{y}{naC^{-1}}\right)\right]+aF\left(\frac{y}{aC^{-1}}\right)-0. \tag{4.2}$$

All but the end terms in the sum cancel, in which case the right-hand side of (4.2) reduces to

$$a \operatorname*{Lim}_{n\to\infty} F\left(\frac{y}{naC^{-1}}\right) = a, \tag{4.3}$$

as required. This verifies that the fluid–fluid interface advances a distance a in a time a/U for all values of y greater than zero. At $y = 0$ this solution does not give any motion since the contribution from the rapid jump at $t = a/U$ is not included.

Solution at large y

We now determine the large-y behaviour of $\phi(y, t; C)$ as given by (4.1). By large y, we mean that y is much greater than aC^{-1}, and we restrict ourselves to this limit. First consider an informal calculation to determine the nature of the large-y behaviour, followed by a discussion of a numerical verification of the procedure (see also Appendix B). The numerical calculation also provides the value of a coefficient that is beyond the scope of the first method. We use the fact that the similarity function F is such that $F(0) = 1$ and $F(x) \to 0$ as $x \to \infty$. Though this calculation is by no means rigorous, it is informative and the result is checked numerically and supported by Appendix B.

It is easier to work with $\phi_y(y, t; C)$ than $\phi(y, t; C)$. From (4.1) we find

$$\phi_y(y,t;C) = a \sum_{n=1}^{\infty} \left[\frac{F'(y/(\gamma t/\mu + naC^{-1}))}{\gamma t/\mu + naC^{-1}} - \frac{F'(0)}{naC^{-1}}\right] + \frac{a\mu}{\gamma t} F'\left(\frac{\mu y}{\gamma t}\right), \tag{4.4}$$

for $0 \leqslant t < a/U$.

Inspection of (4.4) reveals that the dominant contribution to the sum is for n in the range $1 \leqslant n \lesssim y/aC^{-1}$). For n in this range the factors $\gamma t/\mu + naC^{-1}$ are approximately naC^{-1}, which implies that $\phi_y(y, t; C)$ is independent of t for large y. Thus

$$\begin{aligned}\phi_y(y,t;C) &\sim \phi_y(y,0;C) \\ &= C \sum_{n=1}^{\infty} \frac{[F'(y/naC^{-1}) - F'(0)]}{n} \quad \text{as} \quad y/aC^{-1} \to \infty.\end{aligned} \tag{4.5}$$

The term in square brackets in (4.5) is approximately equal to $-F'(0)$ for n much less than y/aC^{-1}, and tends to zero as n tends to infinity. Since the sum of n^{-1} from 1 to N is asymptotic to $\log(N)$ as $N \to \infty$, we can determine the right-hand side of (4.5), to leading order, by truncating the sum at n of the order y/aC^{-1}; the precise point of truncation does not matter. This implies, from (4.5), that

$$\phi_y(y,t;C) \sim C[-F'(0)]\left(\log\left(\frac{y}{aC^{-1}}\right) + k\right), \tag{4.6}$$

where k is an order-unity constant; this is the constant that we determine numerically to complete the matching condition for the outer flow, and is given in terms of F in (B 4). Equation (4.6) is of the same form as for the 'slip models' of Dussan V. (1976), and enables us to define the effective 'slip length' for the current model as aC^{-1} (to an order of magnitude). Dussan V. (1976) has shown that an equation of the form of (4.6) is all that is required to determine the macroscopic flow field.

If we determine the large-y behaviour of $\phi_y(y, t; C)$ numerically we find that the constant k of (4.6) has the value $\log(1/0.140)$, which means that (4.6) can be rewritten as

$$\phi_y(y,t;C) \sim C[-F'(0)] \log\left(\frac{y}{0.140\, aC^{-1}}\right). \tag{4.7}$$

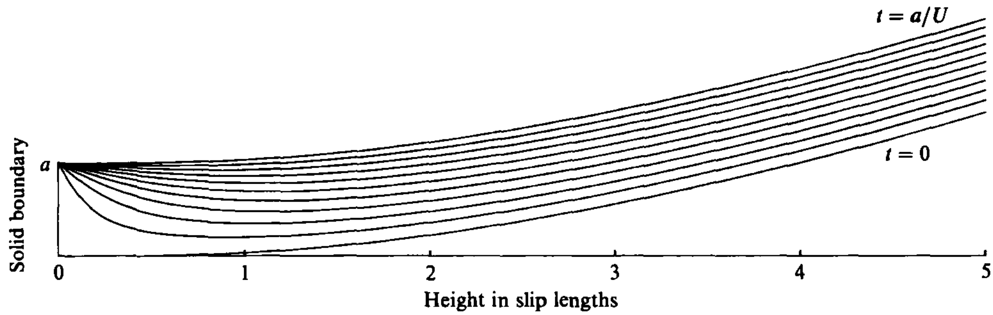

FIGURE 3. The fluid–fluid interface shape at equal time intervals over one period. Note that in this figure a has been taken equal to $\frac{1}{2}L_{\text{slip}}$; this makes the slope of the interface appear larger than in practice.

This seems to indicate that a good definition of the effective 'slip length', L_{slip} is $0.140\,aC^{-1}$.

The numerical solution for the fluid–fluid interface shape in the neighbourhood of the contact line over one period of the motion is shown in figure 3. This figure has been scaled so that a is equal to $\frac{1}{2}L_{\text{slip}}$, which makes the slope of the interface appear larger than in reality (since the theory is valid only when a is much less than L_{slip}). Even at a height of $5\,L_{\text{slip}}$ the motion of the fluid–fluid interface is almost steady, though the distance between the first and second curves is slightly larger than between subsequent curves. However, in the limit of large height the motion of the fluid–fluid interface is steady, and the interface shape tends to that of the 'slip models' of Dussan V. (1976) if the 'slip length' is chosen suitably).

Note that even though the time-dependent solution considered here is non-singular, its time average, to leading order, is the classical solution (B 4) and therefore is singular at the contact line. (In Appendix B this observation is used to determine $F'(0)$.) The singularity in the current model is part of the rapid jump, and so the nature of the rapid jump does not determine the matching condition, to leading order, for the macroscopic flow field for a sufficiently 'slowly moving' contact line. However, details of the rapid jump do determine what is meant by 'slowly moving'. *The reason we can determine the matching condition for the outer flow is that the contact-angle boundary condition is satisfied*; this is not possible if we attempt to use the time-averaged solution, even though it has the same limiting behaviour for large y. The key is to isolate the singularity at the contact line in the rapid jump, which a model assuming steady motion of the fluid–fluid interface could never do.

5. Surfaces with two-dimensional random roughness

Consider the motion of a fluid–fluid interface over a surface with two-dimensional random roughness. Jansons (1985) assumed solid surfaces to be flat except for a random array of isolated rough patches that covered only a small area fraction of the solid, and considered the wetting dynamics theoretically in the limit of zero ϵ. Though these surfaces are only idealizations, they do show many of the observed characteristics of real surfaces, for example contact-angle hysteresis and the stick-slip phenomenon. The size of the jumps in the stick-slip motion of the contact line is on a scale large compaed with roughness dimensions and depends on a 'macroscopic' lengthscale.

We expect the wetting behaviour of these surfaces to be similar to one-dimensional periodic surfaces, since both exhibit contact-angle hysteresis (and stick-slip). In §4 we determined the matching condition for a macroscopic flow without knowing the mechanism of contact-line movement; this was possible because the viscous stress singularity was isolated in the rapid jump. If stick-slip is present the minimum energy dissipation for a contact line moving over a given area must be non-zero, since however slowly the interface moves far from the contact line the motion at the wall will undergo rapid jumps. Each rapid jump dissipates a finite energy that is determined, to leading order, by the roughness and not the mean speed of the contact line. (This is how stick-slip and contact-angle hysteresis are linked.)

For surfaces with random roughness the *area* covered by a rapid jump of the contact line is itself a random quantity. At zero ϵ the average area covered (to an order of magnitude) is

$$a_{\mathrm{p}}\, c \log \frac{1}{c} \mathbb{L}, \tag{5.1}$$

where a_{p} is a typical dimension of a rough patch, $\mathbb{L}$ is a 'macroscopic' lengthscale (e.g. the size of the entire drop) and c is the area fraction of rough patches (Jansons 1985). However, in the limit of small (but finite) ϵ, from an inspection of Jansons' analysis it is clear that the 'macroscopic' lengthscale must be replaced by the lengthscale of the quasi-static neighbourhood of the contact line, namely the effective slip length L_{slip}. Thus (5.1) becomes

$$a_{\mathrm{p}}\, c \log \frac{1}{c} L_{\mathrm{slip}}. \tag{5.2}$$

To determine L_{slip} explicitly we need to know the 'typical' forward displacement b of the contact line in a rapid jump rather than the area covered; since it is b that corresponds to the wavelength of a surface with periodic roughness, i.e.

$$L_{\mathrm{slip}} = \mathrm{b}\mathcal{C}^{-1}. \tag{5.3}$$

However, a determination of b would be complex and may be the subject of future work. For now we shall note that (5.2) suggests that b (considered as a function of L_{slip}) is such that

$$\frac{b(L_{\mathrm{slip}})}{a_{\mathrm{p}}} \rightarrow \infty$$

and

$$b(L_{\mathrm{slip}}) = o(L_{\mathrm{slip}}) \tag{5.4}$$

as $L_{\mathrm{slip}} \rightarrow \infty$. This implies that

$$\frac{L_{\mathrm{slip}}}{a_{\mathrm{p}}\, \mathcal{C}^{-1}} \rightarrow \infty \tag{5.5}$$

as $\mathcal{C}$ tends to zero; therefore in this case L_{slip} is *more* velocity-dependent than for surfaces with periodic roughness.

This helps to explain why theories assuming constant 'slip lengths', need 'slip lengths' larger than roughness dimensions to give agreement with experiment (Dussan V. 1976).

6. Conclusions and discussion

The main conclusion is that a fluid–fluid interface moving over a rough solid surface can be described, to leading order in the slowness parameter ϵ, by continuum quantities (except during a rapid jump). Hence the matching condition for a macroscopic flow problem, in this limit, could be determined independently of the mechanisms of contact-line movement because the non-integrable viscous stress singularity could be isolated (in the rapid jump).

The quantity that corresponds to the 'slip length' in the work of others is shown to be velocity-dependent, and proportional to $a\mathbb{C}^{-1}$ for surfaces with one-dimensional periodic roughness. However, it is clear that the analysis becomes invalid if $a\mathbb{C}^{-1}$ is of macroscopic dimensions, and so this gives a *lower bound* on the value of $\mathbb{C}$. Since the effective 'slip length' obtained is much larger than roughness dimensions, the solid surface may be considered to be *flat* in the macroscopic description.

In §4 we showed that if the contact line had been moving at a constant speed for a 'long time', the fluid–fluid interface is described by a sum of similarity solutions (for a contact line that had made one rapid jump). From (4.1) it is clear that the term 'long time' means that the influence of the contact line has reached macroscopic dimensions, namely that the time t is greater than $\mu\mathbb{L}/\gamma$, where $\mathbb{L}$ is a macroscopic dimension of the flow. Thus the analysis is valid for systems where the macroscopic apparent speed of the contact line is time-dependent, provided that the timescale for changes in speed is greater than $\mu\mathbb{L}/\gamma$. However, the analysis could be extended so that changes in speed could be on any timescale greater than $\mu L_{\mathrm{slip}}/\gamma$.

In §5 we argue informally that the velocity dependence of the 'slip length' for a solid surface with two-dimensional random roughness will be stronger than for a surface with one-dimensional period roughness. In the models presented by Dussan V. (1976), which assume a constant 'slip length', the value of the 'slip length' that gives the best fit with experimental results is much larger than roughness dimensions in the limit of small $\mathbb{C}$. The velocity dependence of the 'slip length' on surfaces with two-dimensional random roughness also explains why the jumps in the 'stick-slip' motion of the contact line decreases in size with increasing speed (see (5.2), (5.3) and (5.4)).

In order for the ideas of this paper to be verified it is necessary to extend the analysis of §4 to cover random roughness, as discussed briefly in §5. For experimental purposes a precise equation relating the size of the jumps in the 'stick-slip' motion to the effective 'slip length' would give the best test of th velocity-dependence of the 'slip length', since it enters measured quantities algebraically rather than logarithmically (as is usually the case).

Appendix A. Long-time limit of the relaxation process

We now justify the statement made in §3 that the long-time limit of any disturbance to the fluid–fluid interface that has a fixed contact line at $z = 1$ and $O(y^{-1})$ as y tends to infinity is the similarity solution F.

From (3.5) we find

$$t\frac{\partial\psi}{\partial t} = Y\frac{\partial\psi}{\partial Y}+\frac{1}{4\pi}\int_0^\infty G\left(\frac{Y}{H}\right)\psi_{HH}(H,t)\,\mathrm{d}H, \tag{A 1}$$

where $\psi(Y,t) = \phi(y,t)$ with $Y = \mu y/\gamma t$ and $H = \mu h/\gamma t$. With this transformation, the time-independent solution of (A 1) is the similarity solution. Consider solutions of the form

$$\psi(Y,t) = A(t)\,B(Y), \tag{A 2}$$

then from (A 1) we find
$$\dot{A}+\frac{n}{t}A = 0 \tag{A 3}$$
and
$$nB+YB'+\frac{1}{4\pi}\int_0^\infty G\left(\frac{Y}{H}\right)B''(H)\,\mathrm{d}H = 0, \tag{A 4}$$
where n is the separation constant. From (A 3) we find
$$A(t) = t^{-n} \tag{A 5}$$
and from (A 4) we can show that
$$B(Y) \sim \text{constant } Y^{-n}, \tag{A 6}$$
as Y tends to infinity.

We require that the expansion for ψ be appropriate for any initial condition for the relaxation process. This initial condition is the fluid–fluid interface shape resulting from the rapid jump of the contact line; we also require that the interface has had time to flatten under the action of surface tension so that we can use the linearized governing equations. Even though the rapid jump cannot be modelled by continuum mechanics in a neighbourhood of size δ of the moving contact line, outside this region the effect of the complex physics is equivalent to a distribution of point forces at its boundaries. Using this distribution of point forces and the stress jump at the fluid–fluid interface, by means of a multipole expansion, we could construct an asymptotic series for the far-field velocity distribution. From this far-field velocity distribution the fluid–fluid interface shape could be determined in the limit Y tends to infnity. We would find that the interface shape has an asymptotic sequence Y^{-n} for positive integers n. Hence, together with (A 6), this implies that the separation constant n can be taken as a positive integer.

We can solve (A 4) exactly for integer n in terms of the similarity solutions F, namely
$$B(Y) = t^n\left(\frac{\mathrm{d}}{\mathrm{d}t}\right)^n F(Y). \tag{A 7}$$
This result can be verified directly by substitution. For convenience define
$$F_n(Y) = t^n\left(\frac{\mathrm{d}}{\mathrm{d}t}\right)^n F(Y), \tag{A 8}$$
where $F_0 = F$. Then, if this set of solutions is complete, the general solution is
$$\psi(Y,t) = \sum_{n=0}^{\infty} c_n t^{-n} F_n(Y), \tag{A 9}$$
where the c_n are constant coefficients. This implies that the general solution for $\phi(y,t)$ is
$$\phi(y,t) = a\sum_{n=0}^{\infty} c'_n\left(\frac{\mu a}{\gamma t}\right)^n F_n\left(\frac{\mu y}{\gamma t}\right), \tag{A 10}$$
where the c'_n are dimensionless coefficients determined from the initial conditions. Though I have failed to prove completeness of the solution set, one important necessary condition, which can be proven, is that shifting the origin of time does not change the form of the solution. From Taylor's Theorem we find
$$F_m\left(\frac{\mu y}{\gamma(t-t_0)}\right) = \sum_{n=0}^{\infty}\frac{1}{n!}\left(\frac{-t_0}{t}\right)F_{m+n}\left(\frac{\mu y}{\gamma t}\right), \tag{A 11}$$

for all t_0 and positive integers m. From (A 11) and (A 9) it follows that shifting the origin for time will not change the form of the solution (A 9) but only the coefficients. This is an important result since no obvious origin for t (for the linearized equations) exists.

Assuming completeness of the solution set, from (A 10) we find that in the limit $\gamma t/\mu a$ tends to infinity

$$\phi(Y,t) \sim ac_0' F\left(\frac{\mu y}{\gamma t}\right)\left(1+O\left(\frac{\mu a}{\gamma t}\right)\right) \tag{A 12}$$

and so tends to a multiple of the similarity solution F, as required.

Appendix B. The time time average of $\phi_y(y,t;C)$ and the value of $F'(0)$

Consider the time average of (4.4) over one period of the motion, where we define

$$\bar{\phi}_y(y;C) = \frac{U}{a}\int_0^{\frac{a}{U}} \phi_y(y,t;C)\,\mathrm{d}t, \tag{B 1}$$

namely

$$\bar{\phi}_y(y;C) = U\int_0^{\frac{a}{U}}\left\{\sum_{n=1}^{\infty}\left[\frac{F'(y/(\gamma t/\mu+naC^{-1}))}{\gamma t/\mu+naC^{-1}}-\frac{F'(0)}{naC^{-1}}\right]+\frac{\mu}{\gamma t}F'\left(\frac{\mu y}{\gamma t}\right)\right\}\mathrm{d}t. \tag{B 2}$$

The right-hand side of (B 2) can be simplified by interchanging the order of integration and summation, thus

$$\bar{\phi}_y(y;C) = C\lim_{K\to\infty}\left\{\int_0^{\frac{aK}{U}}\frac{1}{t}F'\left(\frac{\mu y}{\gamma t}\right)\mathrm{d}t - F'(0)\,(\log K+\gamma_{\mathrm{e}})\right\}, \tag{B 3}$$

where γ_{e} is Euler's constant (not to be confused with surface tension). From (B 3) we find

$$\bar{\phi}(y;C) = -C\left\{F'(0)\log\left(\frac{y}{aC^{-1}}\right)-\int_0^{\infty}F''(\eta)\log\eta\,\mathrm{d}\eta+F'(0)\,\gamma_{\mathrm{e}}\right\}; \tag{B 4}$$

compare (B4) with the matching condition (4.6). Equation (B 4) shows that the time-average of the unsteady motion of the fluid–fluid interface is simply the classical (steady) solution, which was to be expected since (3.5) is linear in $\phi(y,t)$.

Equation (B 4) also provides an easy way of determining $F'(0)$. Since (3.5) is linear the time average of a solution is itself a solution. From (4.3) we also know that $\bar{\phi}(y;C) = U$, which gives

$$U = \frac{\gamma}{4\pi\mu}\int_0^{\infty} G\left(\frac{y}{h}\right)\bar{\phi}_{hh}(h)\,\mathrm{d}h. \tag{B 5}$$

Hence, combining (B 4) and (B 5) we find that

$$F'(0) = \frac{-4\pi}{\displaystyle\int_0^{\infty} G(\eta^{-1})\,\eta^{-1}\,\mathrm{d}\eta} = \frac{-8\pi}{\pi^2-4}. \tag{B 6}$$

REFERENCES

BATCHELOR, G. K. 1967 *An Introduction to Fluid Dynamics*. Cambridge University Press.

BLAKE, J. R. 1971 A note on the image system for a Stokeslet in a no-slip boundary. *Proc. Camb. Phil. Soc.* **70**, 303.

DUSSAN V., E. B. 1976 The moving contact line: the slip boundary condition. *J. Fluid Mech.* **77**, 665.

DUSSAN V., E. B. 1979 On the spreading of liquids on solid surfaces: static and dynamic contact lines. *Ann. Rev. Fluid Mech.* **11**, 371.

HOCKING, L. M. 1977 A moving fluid interface. Part 2. The removal of the force singularity by a slip flow. *J. Fluid Mech.* **79**, 209.

JANSONS, K. M. 1985 Moving contact lines on rough surfaces. *J. Fluid Mech.* **154**, 1.

RALLISON, J. M. & ACRIVOS, A. 1978 A numerical study of the deformation and burst of a viscous drop in an extensional flow. *J. Fluid Mech.* **89**, 191.